Received: 19 April 2023 | Revised: 10 July 2023 | Accepted: 25 August 2023

DOI: 10.1002/app.54683

RESEARCH ARTICLE

Applied Polymer SCIENCE WILEY

Co-axial electrospinning of liposomal propolis loaded gelatin-zein fibers as a potential wound healing material

Canan Yagmur Karakas[1] | **Cem Bulent Ustundag**[2] | **Ali Sahin**[3] | **Ayse Karadag**[1]

[1]Food Engineering Department, Chemical and Metallurgical Engineering Faculty, Yildiz Technical University, Istanbul, Turkey

[2]Bioengineering Department, Chemical and Metallurgical Engineering Faculty, Yildiz Technical University, Istanbul, Turkey

[3]Department of Biochemistry, Faculty of Medicine, Marmara University, Istanbul, Turkey

Correspondence
Ayse Karadag, Food Engineering Department, Chemical and Metallurgical Engineering Faculty, Yildiz Technical University, Istanbul, Turkey.
Email: karadaga@yildiz.edu.tr

Funding information
Scientific and Technological Research Council of Turkey, TUBITAK, Grant/Award Numbers: 2211-A, 120O315; Council of Higher Education (CoHE)

Abstract

In this study, propolis extract (PE) was first encapsulated in different liposomal formulations (65–370 nm) with high encapsulation efficiency (68%–93%). The liposomal PE was further embedded in a food-grade gelatin-zein core/shell fiber by using the co-axial electrospinning method. Transmission electron and confocal laser scanning microscopy verified the structure of liposomes and their homogeneous dispersion in fibers. Scanning electron microscopy (SEM) images confirmed the smooth morphologies of core/shell liposomal fibers. The loading of PE in liposomal fibers improved both thermal (differential scanning calorimetry) and textural (elongation at break and tensile strength) properties, and the fibers loaded with more PE provided higher mucoadhesiveness. The PE-loaded fiber showed higher antimicrobial activity against *Staphylococcus aureus*. The incorporation of liposomal PE in fiber enhanced the viability of human skin fibroblast (HFF-1) cells. The adhesion of HFF-1 cells on fiber was demonstrated by SEM, thus PE-loaded liposomal fiber could provide an efficient platform for cell growth. The findings of this study proposed that propolis-loaded liposomal hybrid fibers produced by the co-axial method can be used as a potential wound healing material.

KEYWORDS

cell adhesion, encapsulation, HFF-1, lecithin, mucoadhesion, nanofilm

1 | INTRODUCTION

The skin serves as the body's first line of immune defense against pathogens and environmental factors, and when its integrity is compromised by wounds, it would provide a potential path for various infections. Similar stages of wound healing occur in both oral and cutaneous wounds, but oral wounds heal quickly and leave a few scars with the help of the increased repair response of the oral fibroblast and mouth epithelial cells.[1] Oral wounds are hurtful for patients, who may experience difficulties masticating, swallowing, and talking, which lower the quality of their daily lives. Oral wounds occur in a water-rich environment rich in bacteria, continuously subjected to both endogenous saliva secretion and exogenous water flushing from food or drink, as well as mechanical movements.[2,3] Therapeutic agents administered topically by mouthwashes, films, ointments, or gels generally suffer

from saliva washout, swallowing, and mouth movement, which influences the residence time and drug distribution at the oral wound location.[4] Therefore, the utilization of mucoadhesive systems can maintain prolonged contact of the formulations with the oral mucosa, allowing for a longer duration of absorption.

Propolis, the resinous substance produced by bees to repair and protect their hive, has been explored for its antimicrobial,[5] antioxidant, anticarcinogenic, and wound-healing[6–8] properties, and those properties could be attributed to the presence of polyphenols (flavonoids, phenolic acids, and their esters). The propolis extracts (PEs) have been reported to promote epithelial repair in surgical buccal wounds,[9,10] increase the amount, type, and density of collagen in oral ulcers and dental pulp, and also reduce the production of mast cells in the inflammatory phase of healing in oral surgical wounds.[11] When the patients suffering from oral recurrent aphthous ulcer (RAU) were treated by niosomal propolis-loaded oromuco-adhesive films, the onset of ulcer size reduction in the medicated group was attained within the second and third days, while for the placebo group, no decrease in ulcer size was observed on these days. Half of the patients in the intervention group recorded complete ulcer healing during the first 5 days, while no patients in the placebo group recorded healing of ulcers in the same treatment days.[12] The main drawback of PE in both nutraceutical and pharmaceutical applications is its low water solubility, for example, highly active molecules present in propolis, like caffeic acid phenethyl ester, and most flavonoids are insoluble in water, which plays a crucial role in its therapeutic efficacy.[13] Encapsulation[14,15] can be a solution to the solubility disadvantage of propolis, but the carrier materials used in the encapsulation system should be non-toxic, biodegradable, and biocompatible so that they can be used safely in food and pharmaceutical applications.

Liposome structures are of great interest as encapsulation systems because they are biocompatible, biodegradable, non-toxic, encapsulate both hydrophilic and hydrophobic substances, and have strong adhesion to various cell surfaces.[16] Their most important disadvantages are their low colloidal stability, the leakage of the encapsulated materials to the outside during storage, and insufficient loading for poorly water-soluble nutraceuticals.[17,18] To increase the stability of liposomes, some improvements have been suggested, such as modifying the fat composition of phospholipids, covering the surface of liposomes with polymers,[19] and pulverizing polymer-coated liposomes in the presence of a non-adsorbing carrier material[20,21] and embedding liposomes in film structures.[22,23]

In recent years, the integration of liposomes in electrospun fibers (NFs) has gained substantial attention and shown significant potential for applications in different food and medical fields.[18,24–26] Fibers with high porosity and surface-to-volume ratios enable improved loading capacity and encapsulation efficiency of the active substance, enhanced solubility, and biodegradability.[27] Hasanbegloo et al.,[25] fabricated paclitaxel-loaded liposome-loaded chitosan (core)/poly-ε-caprolactone (PCL)-chitosan (shell) fibers for the treatment of breast cancer and reported decreased tumor weight by the incorporation of liposome in the fibers. As a potential drug delivery system, Mickova et al.[28] incorporated phosphatidylcholine (PC) liposomes into polyvinyl alcohol (PVA) (core)/PCL (shell) fibers to encapsulate an enzyme (horseradish peroxidase), preserve the activity of the enzyme, and enhance stem cell proliferation. Feng et al.[26] produced PVA (core)/alginate- polyethylene oxide (PEO) (shell) fibers embedded with PC liposomes to encapsulate salmon calcitonin-a peptide hormone, and the resulting fibers delayed the release of the peptide in simulated gastric and intestinal fluid. Feritas Zompero et al.[22] incorporated ß-carotene-loaded liposomes into the electrospun fiber of PVA and PEO blends to enhance the UV photostability of carotenoid. Alehosseini et al.[29] embedded curcumin-loaded PC liposomes into the electrospun fiber of zein and gelatin blends, and liposome addition enhanced the solubility of curcumin in protein fibers and promoted the sustained release of curcumin. Zein and gelatin are both natural biopolymers with good biocompatibility, biodegradability, and mucoadhesiveness,[30,31] and the blend of these polymers has been used in the production of electrospun fibers in various applications such as the encapsulation of resveratrol,[32] curcumin,[29] angelica root oil,[33] and *Momordica charantia* fruit extract,[34] for enhanced cell attachment and growth,[35] and for hemostatic dressings.[36]

In this study, the fabrication of soy phosphatidylcholine liposomal propolis (PE) embedded in zein-gelatin fibers by co-axial electrospinning was proposed as a potential wound-healing material with biocompatible and mucoadhesive properties. There have been some studies to encapsulate PE in electrospun fibers in PVA,[37,38] the blend of PVA/PCL,[39] PCL,[40,41] polyamide-6,[42] zein,[43–45] and silk fibroin.[46] However, to the best of the authors' knowledge, no study has dealt with incorporating PE-loaded liposomes within a polymeric core-shell fiber structure. In this respect, the PE-loaded liposome structure and its distribution in fibers were visualized by transmission electron, confocal laser, and field emission scanning microscopy. Scanning electron microscopy (SEM) analysis was used to assess the morphology of the fibers. The electrospun fibers were additionally characterized by Fourier transform infrared (FT-IR) spectroscopy and differential scanning calorimetry (DSC) analysis. In addition to the textural (tensile strength [TS] and elongation at break [EAB]) and in vitro mucoadhesiveness properties, the swelling-degradation characteristics of fibers and the release of PE were determined. To evaluate the liposomal PE-loaded fiber as a wound dressing application, the interactions of the

sample with skin fibroblast cells (HFF-1) were determined by the MTT assay, cell adhesion to fibers was visualized by SEM, and its antimicrobial effect against three aerobic bacterial species commonly encountered in skin wounds was also evaluated.

2 | MATERIALS AND METHODS

2.1 | Materials

Lipoid S75 (70% phosphatidylcholine) was bought from Lipoid (Ludwigshafen, Germany). Propolis extract was kindly donated from Balparmak (Altıparmak Gıda, Istanbul, Turkey). Food-grade zein, kindly gifted from the Flozein company, and fish gelatin (gelatin from cold-water fish skin, Sigma, Canada) were used as polymers in the production of liposomal fibers. Glacial acetic acid (100% anhydrate) and ethanol (99.5%, extra pure) were obtained from Isolab (Turkey) and Tekkim (Turkey), respectively. Nile red, fast green, glutaraldehyde, MTT (3-[4,-dimethylthiazol-2-yl]-2, 5-diphenyltetrazolium bromide; thiazolyl blue), mucin type II (M2378) and Tween 80 were purchased from Sigma Aldrich (Steinheim, Germany).

Our method section comprises three divisions. The first one was the preparation of PE-loaded liposomes and their characterization (EE%, TEM imaging, particle size, and zeta potential values). The second division belonged to the preparation of co-axial liposomal fibers by electrospinning and the characterization of fibers (loading capacity of PE, color, DSC, and FT-IR analysis; imaging by SEM, transmission electron, and confocal laser scanning microscopy; mechanical strength, swelling, and degradation of fibers). The third one concluded some bioactive properties of liposomal PE-loaded core/shell fibers by determining the release of PE, in vitro mucoadhesive and antimicrobial properties, and the viability of human fibroblast cells subjected to fibers and adhesion of cells to fibers.

2.2 | The preparation of liposomes and their characterization

2.2.1 | Preparation of propolis (PE)-loaded liposomes

Empty and PE-loaded liposomes were prepared according to Shao et al.[47] and Karadag et al.[48] with minor modifications. First, 2%–5% (w:v) of lecithin, PE (0.3%–4%, w:v), and Tween 80 (1%, w:v) (Table 1) were dissolved in ethanol with a magnetic stirrer until the mixture was completely homogeneous, and the solvent was removed by using a rotary evaporator (Buchi-R-210, Germany) under vacuum (40°C, 70 mmHg). The dry lecithin-propolis film layer was dispersed in ultrapure water and homogenized by using Ultra-Turrax (IKA T-18, Germany) for 5 min at 10.000 rpm and sonicated (0.5 cycles, 60% amplitude) for 5 min with an ultrasonic processor (UP400S, Hielscher, Germany).

2.2.2 | Particle size and zeta potential of liposomes

The average particle diameter (z average), polydispersity index (PDI), and zeta potential of the liposomes were measured using dynamic light scattering on a Zetasizer Nano ZS (ZEN3601, Malvern). All samples were diluted to 1000 (v:v) fold, and measurements were made on freshly prepared liposomes three times per sample.

TABLE 1 The nomenclature of samples.

	Sample	PE % (w:v)	Lecithin % (w:v)	T80% (w:v)
Liposome	L1	0.3	2	—
	L2	0.6	4	—
	L3	2	5	1
	L4	4	5	1
Fiber		*Embedded liposome*		
	F1	L1		
	F2	L2		
	F3	L3		
	F4	L4		
	EF	—		
	F2B	Blank L2 (PE free)		
	F4B	Blank L4 (PE free)		

Abbreviations: EF, empty fiber (without liposomal PE, only polymers); PE, propolis extract; T80, Tween 80.

2.2.3 | Encapsulation efficiency (EE%) of PE in liposomes

Total phenolic content (TPC) and total flavonoid content (TFC) of PE were carried out using the Folin–Ciocalteu (FC) method Singleton and Rossi,[49] Meda et al.,[50] and Pękal and Pyrzynska,[51] respectively. The TPC values were given as gallic acid equivalent (GAE), and the TFC was calculated in terms of quercetin (QE) equivalent with the help of external standard curves. For the determination of EE%, free PE was separated from the PE-loaded liposomes by centrifuging at 4000 ×g for 40 min. at 4°C using an Amicon® membrane ultra-centrifugal filter (50 kDa).[52] 1 mL of liposome was added to the upper section of the filter, free PE was filtered to the permeate, and the PE-loaded liposomes stayed in the retentate phase. The amount of free PE in the permeate could be lower for detection with the spectrophotometric assay; therefore, both phases were measured to determine the EE% of PE. The retentate phase was mixed with ethanol and centrifuged at 4000 ×g for 30 min at 4°C to precipitate the lecithin, and the supernatant was used for PE determination. The blank liposome (with no PE) was also processed similarly as a blank for spectrophotometric assays. The calculation was given based on the PE in retentate (upper section), but the values were also verified by the calculation of free PE in the lower section of the Amicon filter.

$$\mathrm{EE}\% = \frac{\text{Amount of PE (TPC or TFC) recovered from retentate}}{\text{Amount of PE (TPC or TFC) loaded initially}} \times 100$$

2.2.4 | Transmission electron microscopy imaging of liposomes

An amount of liposomal solution was put on carbon-coated copper grids (200 mesh) and waited until it was completely fixed at room temperature. The grid was then stained with a 2% uranyl acetate aqueous solution and dried at room temperature. The image of liposome structure was taken by TEM (Hitachi HT7800, Tokyo, Japan), operating at 100 kV of acceleration voltage equipped with a digital camera.

2.3 | Preparation of co-axial liposomal fibers by electrospinning

A mixture of zein and gelatin (3:1, w:w) was dissolved in an acetic acid solution (80%, w:v) at a concentration of 40% (w:v). The inner syringe solution consisted of liposomes (blank or PE-loaded) and previously a prepared zein-gelatin solution at a ratio of 3:7 (v:v). The outer syringe was filled only with zein-gelatin (3:1, w:w) solution (40%, w:v). The electrospinning process was carried out in the electrospinning device (Holmarc Opto Mechatronics Pvt. Ltd. India model no: HO-NFES-0434). The process parameters were as follows: 17 kV voltage, 0.5 mL/h flow rate of an external solution on the outer syringe (15G–1.829 mm) and 0.1 mL/h internal fluid on the inner syringe (21G–0.819 mm), the distance between the collector plate and the nozzle was 12 cm, and the current was 5 mA. All studies were carried out at room temperature (25°C) and around 50% relative humidity in the chamber.

2.3.1 | Loading amount of PE in liposomal fibers

Approximately 0.5 g of fibers were mixed with 2 mL of 80% acetic acid solution in a shaker (150 rpm) overnight until the fibers were completely dissolved. It was mixed with ethanol at a ratio of 1:1 (v:v), and centrifuged at 7800 ×g for 15 min at 4°C. TPC content was determined in the supernatant for each g of fiber.

2.3.2 | Surface color of fibers

Color analysis of fibers was performed using a colorimeter (Model CR-400, Konica Minolta Sensing, Inc., Osaka, Japan). The L (lightness), a* (redness/greenness), and b* (yellowness/blueness) parameters were determined to evaluate the color of the fibers. At least eight replicates were carried out per fiber. The total color difference (ΔE) parameter was calculated according to the following formula. The empty fiber (without liposomal PE, only polymers) was used as a reference film in the ΔE calculation.[53]

$$\Delta E = \sqrt{(L* - L)^2 + (a* - a)^2 + (b* - b)^2}$$

2.3.3 | Texture analysis of fibers

The mechanical strengths of the fibers were determined using a Texture Device (Stable Micro System, TA-XT2Plus, UK) with a 5 kg load cell. The fibers were cut into 1 mm-thick strips (60 mm × 10 mm) and tested at ambient temperature. The mean value was calculated from the six measurements made on each sample.[35]

2.3.4 | Morphological analysis of fibers by SEM and confocal laser microscopy

For SEM analysis, all samples were spray coated with a thin layer of gold-platinum (Agar Manual Sputter Coater

B7340, Agar Scientific, Stansted, UK) under a vacuum using a current density of 40 mA. The morphology of the fibers was analyzed by SEM (FEI Quanta 450 FEG, Graz, Austria), under a low vacuum, a distance of 6.5 mm, and an acceleration voltage of 10 kV. To examine the average diameter of fibers (100 samples), Image J software (National Institutes of Health) was used. The fibers were also analyzed by field emission scanning microscopy (FE-SEM) with a scanning transmission electron microscopy (STEM) detector (Thermo Scientific Apreo 2 S LoVac) to visualize the core/shell structure. Fiber imaging was also performed on a confocal laser microscope (Zeiss LSM 780, Carl Zeiss, Oberkochen, Germany) controlled by Zeiss Zen Software (2012 SP1 black edition). Liposomes were stained with Nile red, an oil-soluble dye, and the protein-polymer phase was stained with Fast green. Nile red and Fast green dyes were dissolved in a certain amount of ethanol and dripped onto the liposome and polymer mixture prior to the manufacturing of fibers.

2.3.5 | Differential scanning calorimetric analysis of fibers

The thermal properties of the fibers were obtained using DSC (SDT Q600, TA Instruments, New Castle, DE) under nitrogen gas flow. Each sample (5–8 mg) was accurately weighed into aluminum containers and hermetically sealed. Sealed samples were heated at 20°C min^{-1} from 20 to 500°C under a nitrogen flow of 20 mL/min.

2.3.6 | Fourier transform infrared spectra of fibers

Fourier transform infrared spectra of the fibers were obtained using an FTIR spectrophotometer (ATR-FTIR; Bruker Tensor 27, Karlsruhe, Germany). All spectra were recorded in absorption mode at a resolution of 4 cm^{-1} at wavelength range of 4000–500 cm^{-1}.

2.3.7 | Swelling and degradation analysis of fibers

The swelling and degradation characteristics of the fibers were determined by monitoring the mass changes during incubation. A 40 mg of fibers were dipped in 20 mL of phosphate buffer (PBS, pH 7.4) and acetate buffer (AB, pH 4.5) and kept at constant temperature and agitation (37°C, 70 rpm). Swollen fibers were taken at certain times and weighed (W_a) immediately after removing excess liquid from the surfaces. By determining the ratio of fibers to their initial weight (W_i), the swelling ratio (SR%) was calculated:

$$SR\% = \frac{W_a - W_i}{W_i} \times 100$$

At the specified times, the fibers were removed and allowed to dry, and the weights of the dried films were determined (W_t). The degradation ratio (DR%) was determined using the formula:

$$DR\% = \frac{W_t}{W_i} \times 100$$

SEM analysis (Section 2.3.4) was used to observe the morphology of PE-loaded liposomal fiber immersed in PBS and AB for 15 min, 1 h, 6 h, and 24 h.

2.4 | The bioactive properties of liposomal PE-loaded fibers

2.4.1 | The release (%) of PE from fibers

The release (%) of PE from the liposomal fibers was determined in PBS (pH 7.4). The fiber with the highest PE loading (F4) was selected for the analysis. 60 mg of sample were put in the tubes with 20 mL of PBS for each time interval, and the tubes were incubated in a thermal shaker (37°C, 250 rpm), and the content of the tubes taken at 1, 2, 4, 6, 8, and 24 h of incubation was analyzed by the Folin–Ciocalteu (FC) method as stated in Section 2.2.3.

2.4.2 | In vitro mucoadhesive properties of fibers

The mucoadhesion of fibers was determined by measuring the adhesion force (N) and work of adhesion (N mm) on a texture analyzer TA-XT2 (Stable Micro-Systems) with 5 kg of a load cell, in the adhesive mode, using porcine mucin discs as a substrate.[54,55] Mucin discs were prepared with a hydraulic pressure machine by applying 10 tons for 30 s. The fibers adhered to the P/10 probe (10 mm), and the mucin discs were attached to the metallic holder with double-sided adhesive tape. The mucin discs were previously hydrated with 0.1 M PBS (pH = 7.4) for 60 s, the excess solution was withdrawn with an absorbent paper. The probe was lowered towards the metallic holder until the fibers reached the disc surface at a speed of 0.5 mm/s, and contacted the mucin disc

by applying 5 kg of force for 100 s. After, the probe was lifted at a constant speed of 0.5 mm/s, to promote the complete detachment of the fiber from the mucin disc. Analyses were performed in six replicates. Mucoadhesion work was calculated from the force-distance graph by using the device software.

2.4.3 | Antimicrobial activity of fibers

The antibacterial activity of liposomal PE-loaded fiber (F4) was tested against *Staphylococcus aureus* (Gram-positive, ATCC 29213), *Escherichia coli* (Gram-negative, ATCC 25922), and *Pseudomonas aeruginosa* (Gram-negative, ATCC 27853), which have been reported as aerobic bacteria commonly encountered in skin wounds. The blank-liposome loaded fiber (F4B) was used as a control, and the antimicrobial activity was determined by an agar diffusion test. Fibers were sterilized with UV light for 5 min. before analysis. Briefly, the bacterial suspension (100 μL, 10^7 CFU/mL) was spread on petri dishes of nutrient agar, and fibers were placed. After 24 h of incubation at 37°C, the clear region formed around the fiber was measured to assess the inhibitory effect. Each test was repeated three times under the same conditions.

2.4.4 | MTT assay for cell viability

Cytotoxicity analysis of liposome-loaded fibers (F3, F4, and F4B) was determined by the indirect contact method.[56] For the indirect assay, fibers of the same size were sterilized for 1 h using UV radiation and kept in a cell culture medium (DMEM) for 24 h. The effect of the medium on cell viability was tested on HFF-1 (human fibroblast, ATCC SCRC1041) cells seeded in the 24-well plates. After 24 h of the incubation period, the standard MTT (3-[4,-dimethylthiazol-2-yl]-2, 5-diphenyltetrazolium bromide; thiazolyl blue) test was performed, and the percentage of cell viability was calculated according to the formula:

$$\text{Cell viability}\% = \frac{\text{OD}_{\text{sample}}}{\text{OD}_{\text{control}}} \times 100$$

2.4.5 | Cell adhesion analysis in SEM

For cell adhesion testing, liposomal PE-loaded fiber (F4) was placed in wells after being sterilized under UV radiation for 1 h, and HFF-1 fibroblast cells were seeded into each well of 24-well flat bottom microplates at a number of 5×10^4 in 1 mL medium and incubated at 37°C for 24 h for cell attachment. After a 24-h incubation period, cells were fixed on the fiber with a 2.5% glutaraldehyde solution and purified by passing through a series of ethanol solutions (30%, 50%, 70%, 80%, and 95%) for SEM analysis (Section 2.3.4).

2.4.6 | Statistical analysis

All experiments were carried out in triplicate, and the results were given as the mean ± standard deviation. Statistical analysis was performed with SPSS Statistics Software (IBM version 20, Armonk, NY). The differences between the mean values were evaluated using a one-way analysis of variance (ANOVA), followed by Tukey's post hoc test. Differences were considered significant if $p < 0.05$.

3 | RESULTS AND DISCUSSION

3.1 | Particle size, morphology, and encapsulation efficiency (EE%) of liposomal PE

The particle size and zeta potential values of PE-loaded liposomes were given in Table 2. The lecithin to PE ratio in the L1 and L2 formulations was the same (6.7:1, w: w), and increasing the PE loading further in those formulations caused precipitates. Liposomes were known for their insufficient loading for poorly water-soluble nutraceuticals.[18] Therefore, to enhance the PE loading, Tween 80 was added to the formulation of L3 and L4 (Table 1), and excipient also used in liposome production.[57] The combination of phospholipids with other emulsifiers has suggested some unique advantages, such as enhanced drug solubility and loading performance. Li et al.,[58] reported that inclusion of Tween 80 enhanced the encapsulation efficiency of curcumin from 50.43% to 80.12% in soybean PC liposomes. Tan et al.,[59] prepared liposome-containing carotenoids with the combination of Tween 80 and egg yolk PC to overcome the poor solubility of lycopene, β-carotene, and lutein. The blank propolis-free liposomes of L2 and L4 had a size of 64.61 ± 16.43 and 387.8 ± 62.62 nm, respectively. The presence of Tween 80 in the liposome formulation significantly increased the particle size. Xia and Xu,[60] suggested that at low concentrations (<0.8 molar ratio; Tween 80: lipids), the surfactant molecules could be adsorbed by the lecithin membrane without breaking up the liposome structure. The addition of surfactants to liposomal systems was also done to alter the structure of the membranes to provide more space for encapsulation.[61] The size of the liposomes produced with surfactant was also higher in the study of

TABLE 2 The particle size, polydispersity index (PDI), surface charge (zeta potential), and encapsulation efficiency (EE%) values of liposomal PE formulations.

Sample	Size (nm)	PDI	Zeta potential (mV)	EE of PE%	
				TPC	TFC
L1	69.14 ± 0.43^{c}	0.24 ± 0.00^{c}	-33.06 ± 0.68^{ab}	93.04 ± 0.22^{a}	98.24 ± 0.35^{a}
L2	64.36 ± 4.22^{c}	0.23 ± 0.03^{c}	-32.10 ± 1.10^{ab}	94.16 ± 0.41^{a}	97.84 ± 0.01^{a}
L3	261.50 ± 18.39^{b}	0.39 ± 0.03^{b}	-33.23 ± 0.38^{b}	89.70 ± 1.86^{a}	85.82 ± 2.91^{b}
L4	370.46 ± 35.28^{a}	0.53 ± 0.03^{a}	-30.93 ± 1.11^{a}	68.01 ± 4.94^{b}	76.23 ± 3.46^{b}

Note: Values were presented as mean ± SD ($n = 3$). Values with different superscript lowercase letters within the same column were significantly different ($p < 0.05$).
Abbreviations: PE, propolis extract, TFC, total flavonoid content; TPC, total phenolic content.

Romana et al.,[62] who showed that the surfactant micelles were also loaded inside the aqueous core of liposomes. Between L1 and L2, in which the mass ratio of lecithin to PE was constant (6.7:1, w: w), the particle size and polydispersity index (PDI) did not change significantly ($p > 0.05$). The mass ratio lecithin to PE (w:w) was reduced from 2.5 to 1.25 from L3 to L4, meaning that the L4 formulation had less phospholipid bilayer for the same amount of PE. Due to its hydrophobic nature, PE was expected to be more embedded inside the bilayers, so it can be deduced that higher incorporation of PE would lead to larger liposomal vesicles since there was less surface to interact with in the L4 formulation. The studies related to liposomal propolis production also reported a larger size of liposomes depending on the higher PE loading at constant lecithin concentrations.[63,64]

The higher zeta potential values of blank L2B (-39.23 ± 1.15 mV), and L4B (-34.10 ± 0.60 mV) could suggest that PE also interacted with the surfaces due to the lower zeta potential values of PE-loaded liposomes (Table 2). There have been studies stating that many phenolic compounds interact with liposome structures through hydrophilic and hydrophobic interactions.[65,66] The low PDI value is a measure of the size-based heterogeneity of a given sample, higher PDI values show that the homogeneity of the liposome size distribution decreases, and higher PE loading decreased the homogeneity of our liposomal dispersions (Table 2). The negative staining with uranyl acetate was done to create a contrast that would allow the visualization of liposome spherical structures by TEM analysis. The presence of spherical liposomes (white arrows) can be seen in the images of PE-loaded and blank liposomes (Figure 1).

Very high EE% values of PE (over 90% in TPC and 95% in TFC) were determined in L1 and L2 liposomes in which the mass of PE was lower (0.3% and 0.6%, w:v). It has been widely accepted that molecules with high hydrophobicity are easier to embed into the phospholipid bilayers through steric fitting and hydrophobic interactions, and polyphenols could also be absorbed on the surface of liposomal vesicles due to the abundance of hydroxyl groups.[61] Between L3 and L4, at the constant lecithin content, EE% decreased from around 90% (in TPC) to 70%, upon the increase in PE loading from 2% to 4% (w:v). The lower EE% in L4 could be the result of the less available liposomal surface for PE to interact with compared to L3, and some of the PE might be suspended in the surfactant micelles in the aqueous phase. In the liposomal systems, the decreased EE% values with the increased amount of loaded material at the constant lecithin concentrations were also previously reported for the extracts of PE,[63] black mulberry,[48] black carrot,[67] and quercetin.[68] Yuan et al.[69] produced liposomes by ethanol injection and membrane filtration and determined EE% values of propolis between 76% and 93%.

3.2 | The color, textural properties, PE loading, and morphology of liposomal fibers

In addition to fibers (F1–F4) embedded with L1–L4 formulations, we also produced empty fibers with no liposome (EF), and fibers filled with blank liposomes (F4B) to evaluate the influence of PE and liposome loading. Production of fibers with only PE loading was not possible because PE cannot be solubilized in the solvent (water and the acetic acid solution) used for the dissolution of our polymers, gelatin, and zein. L*, a*, and b* values of EF and F4B fibers were very similar, the incorporation of liposome increased (2.02–2.71) the yellowness (b* value) ($p < 0.05$) (Table 3). The PE was naturally dark brown, and the zein was yellow in color.

The other color parameters were in a similar range among fibers, therefore the main contribution to the total color difference (ΔE) was derived from the b* value. When comparing the F4 liposomal with its blank (F4B), loading PE significantly elevated the b* value

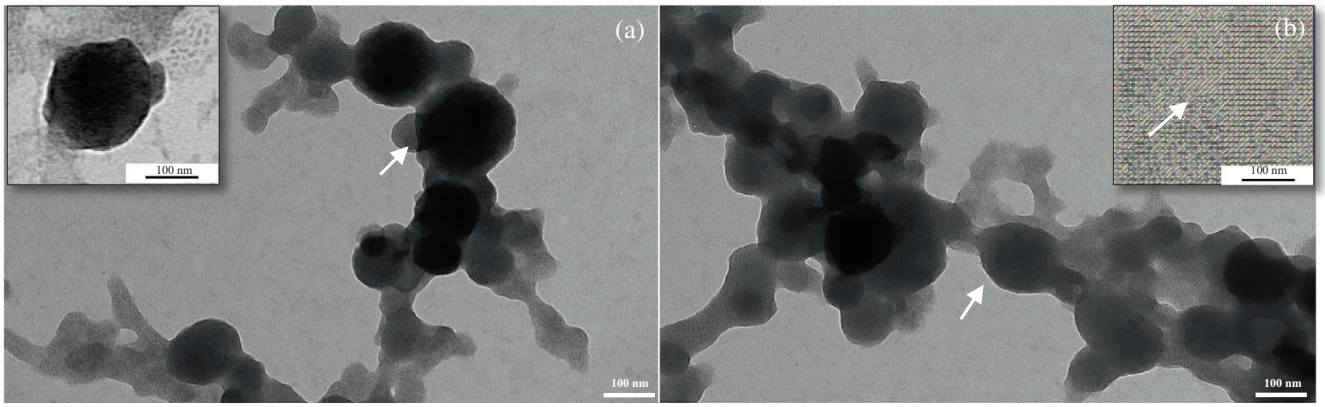

FIGURE 1 Transmission electron microscopy images of (a) propolis extract (PE)-loaded liposome, (b) blank-PE free liposome (scale bars indicates 100 nm). [Color figure can be viewed at wileyonlinelibrary.com]

TABLE 3 Total phenolic content (TPC), propolis extract (PE) loading, and color of fibers.

Sample	L*	a*	b*	Δ*E*	TPC (μg GAE/g fiber)	PE (μg/g fiber)
F1	95.97 ± 0.07^{a}	-0.59 ± 0.01^{a}	2.80 ± 0.10^{b}	1.20 ± 0.30^{a}	93.1 ± 1.40^{c}	332.20 ± 4.99^{d}
F2	95.82 ± 0.1^{ab}	-0.62 ± 0.04^{ab}	3.07 ± 0.29^{ab}	1.41 ± 0.23^{a}	198.3 ± 2.5^{c}	707.58 ± 8.92^{c}
F3	95.30 ± 0.18^{bc}	-0.69 ± 0.01^{bc}	3.28 ± 0.18^{a}	1.34 ± 0.21^{a}	752.5 ± 3.5^{b}	2685.10 ± 12.48^{b}
F4	95.52 ± 0.2^{abc}	-0.72 ± 0.01^{c}	3.48 ± 0.08^{a}	1.55 ± 0.13^{a}	1710.7 ± 4.7^{a}	6104.19 ± 16.77^{a}
EF	95.08 ± 0.36^{c}	-0.69 ± 0.02^{bc}	2.02 ± 0.02^{c}	—	—	—
F4B	95.14 ± 0.13^{c}	-0.65 ± 0.04^{abc}	2.71 ± 0.08^{b}	0.72 ± 0.10^{b}	—	—

Note: F1–F4: fibers loaded with liposomal PE (L1–L4). EF: empty fiber (without liposomal PE, only polymers); F4B: fiber loaded with blank-PE free L4 liposome; Δ*E*: Total color difference; GAE, gallic acid equivalent. Values were presented as mean ± SD ($n = 3$). Values with different superscript lowercase letters within the same column were significantly different ($p < 0.05$).

(from 2.71 to 3.48), the higher yellowness of fibers complied with the higher PE (TPC) loading per gram of fiber. The photographs of F4 and F4B were additionally given in Figure 3. A 1 g of F4 and F3 liposomal fiber contained 1710 and 752 μg GAE which corresponded to 6.1 and 2.7 mg of PE, respectively. Although the loading of PE in the F3 fiber was lower than that in the F4, the difference in the *b* value was not significant ($p > 0.05$).

Tensile strength and EAB are parameters related to the mechanical properties of fibers (Figure 2). The oral wound dressings should have an appropriate mechanical strength to withstand the breakage caused by possible external impacts (chewing, talking, swallowing, movement of the tongue, etc.) in the dynamic oral environment.[70,71]

When the PE-free liposomal fibers (F2B and F4B) were compared (Figure 2), the higher lecithin content and inclusion of Tween 80 of the liposome formulation embedded in the fiber elevated the TS of the samples. The plasticizing effect of Tween 80 may affect the interpolymer interactions by increasing the free volume between chains of polymers,[72] although it was reported that the presence of plasticizer reduced the TS value of films, this property would depend on the final concentration of the surfactant. When the final amount of plasticizer in the polymeric material was low or high, there might be few or excessive interactions, respectively, so TS could be increased.[73] The type of plasticizer was also important in the mechanical properties of the films; for example, the addition of soy lecithin at a concentration of 5%–15% in zein films was reported to increase the TS values due to its hydrophobic nature.[74]

The difference in TS value between the blank liposomal fibers and their PE-loaded counterparts (F2B and F2; F4B and F4) indicated that PE loading reduced the TS of the samples. The decrease in the TS values may indicate the decreased densification of networks and weakened intermolecular forces of polymers and generally decrease stiffness and improve the flexibility and elasticity of fibers, allowing larger deformation under weak intermolecular interactions, which reflect the increase in EAB value.[58] All liposomal fibers, except F4B, had significantly higher ($p < 0.05$) EAB values compared to fibers without liposome and propolis (EF). Similarly, Ge et al.[75] and Li et al.,[58] produced liposomal fibers and both reported that the incorporation of liposomes enhanced the EAB values of fibers.

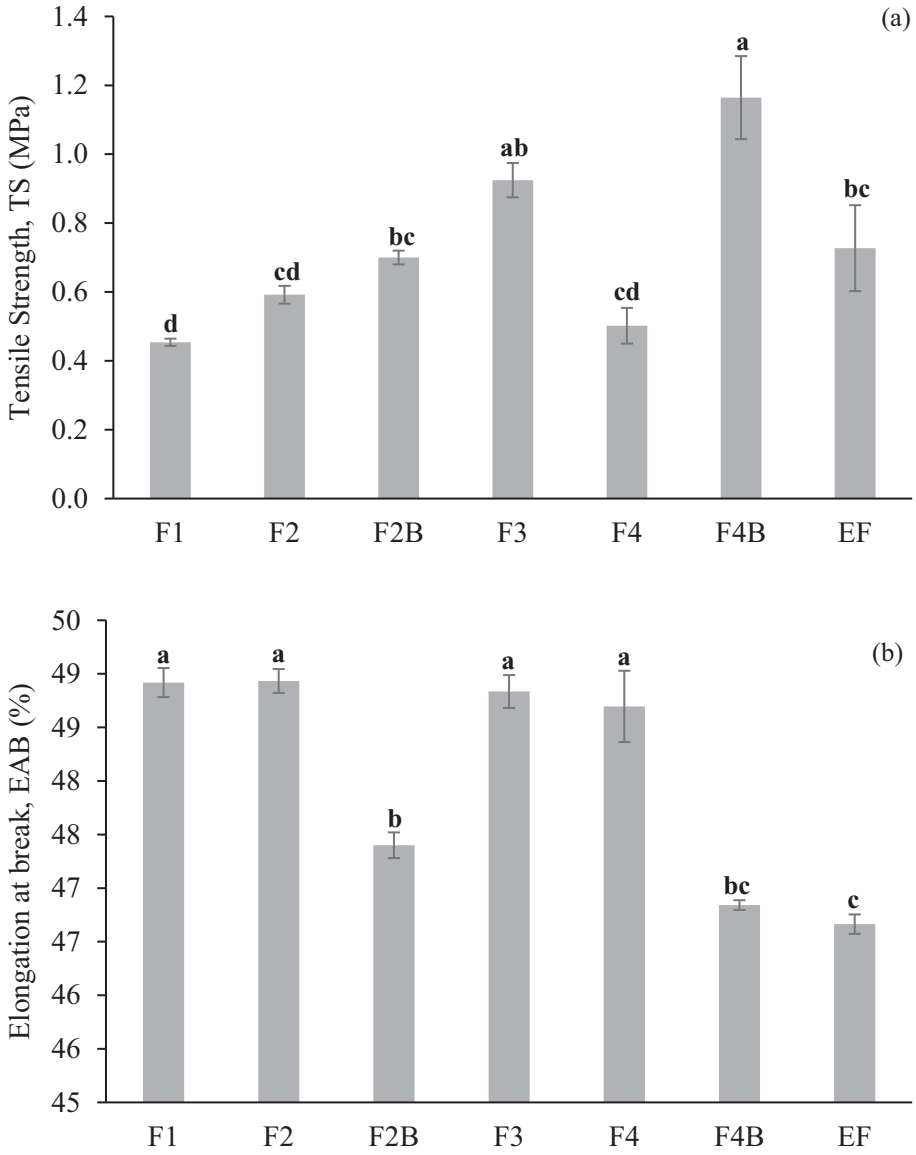

FIGURE 2 Tensile strength, TS (MPa) (a), and elongation at break, EAB (%) (b) values of fibers. F1–F4: fibers loaded with liposomal propolis extract (PE) (L1–L4). EF: empty fiber (without liposomal PE, only polymers); F2B: fiber loaded with blank-PE free L2 liposome; F4B: fiber loaded with blank-PE free L4 liposome. Values are presented as mean ± SD ($n = 6$). Means with different letters are significantly different ($p < 0.05$).

In our samples, this value was always higher in PE-loaded liposomal fibers (F1–F4) compared to PE-free liposomal samples (F2B and F4B). PE is composed of resin, wax, and other hydrophobic components in addition to phenolic substances. The addition of liposomes containing PE likely resulted in reduced interaction between gelatin and zein monomers and inhibition of polymer chain-chain interactions, leading to lower TS concomitant with an increase in EAB of the fibers. Eskandarinia et al.[6] also found that propolis-containing cornstarch films had lower TS and higher EAB values. Adding hydrophobic compounds to the polymer network could form a heterogeneous structure and discontinuous areas in the fiber, which would eventually lead to decreased TS of the film.[32] In FT-IR analysis of our samples (Figure 6), the peaks observed at 1633 and 1512 cm^{-1} in PE manifested themselves at 1652 and 1538 cm^{-1} when it was embedded in gelatin-zein fiber, which could be an indication of interaction between PE and polymers that leads to alterations in the textural properties. It can be concluded that the embedding of liposomal PE in gelatin-zein fibers decreased both TS and increased EAB values, therefore improving the mechanical properties and making them more resilient to external stresses during their handling by both producers and consumers.

As was seen in SEM images (Figure 3), the liposomal fibers have a smooth surface and uniform morphology. The presence of only a few beads (white arrows) can be realized, which was a very common defect in electrospun fibers, and their incidence could be reduced by optimizing process parameters. By comparing the surface morphology of fibers, no distinguished difference was observed, so the addition of blank and PE-loaded

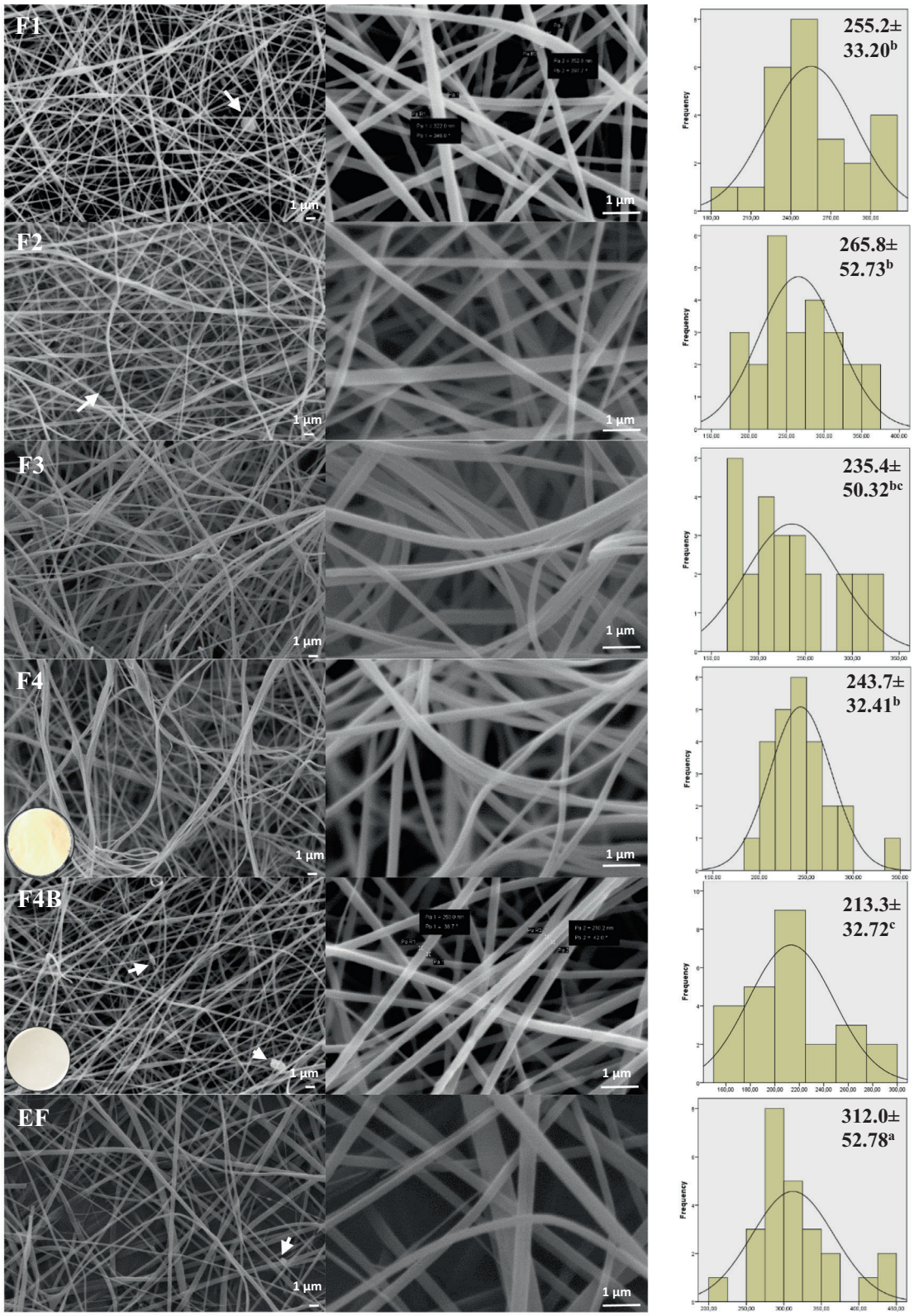

FIGURE 3 Scanning electron microscopy images (left), the diameter distribution of electrospun fibers (right), and the representative photos of liposomal fibers (F4 and F4B). F1–F4: fibers loaded with liposomal propolis extract (PE) (L1–L4); F4B: fiber loaded with blank-PE free L4 liposome; EF: empty fiber (without liposomal PE, only polymers). [Color figure can be viewed at wileyonlinelibrary.com]

liposomes did not cause structures that would indicate the incompatibility of polymers and the phase separation of the feed solution. The size of empty fiber, EF, was the largest (312.0 ± 52.78 nm), and liposome loading significantly reduced the size in F4B (213.3 ± 32.72 nm) ($p < 0.05$). Liposomal PE-loaded fiber (F4: 243.7 ± 32.12 nm) was slightly larger ($p < 0.05$) than its blank counterpart (F4B). The size of liposomal fibers (F1: 255.2 ± 33.20 nm, F2: 265.8 ± 52.73 nm), in which the liposome did not have Tween 80 in formulation, was higher than those of F3 and F4, and PE loading alone may not be a significant factor. It can be concluded that incorporating liposomes into empty fibers independent of the presence of PE reduced fiber size, and lecithin and T80 acted as plasticizers, improved the electrospinability of the polymer solution, and resulted in smaller-sized fibers.[26] Similarly, when Cui et al.[76] added tea-tree oil-loaded liposomes to chitosan fibers, the size of the fibers decreased from 151 to 135 nm.

The lecithin and polymers were stained with two different fluorescent dyes (Nile red and fast green, respectively) prior to the liposome production and electrospinning process, and the images of liposomal fiber were taken with a confocal laser microscope (CLSM). In Figure 4a–c, the 2D and 3D CLSM images of fibers were given. Liposome vesicles (green) in fiber can be distinguished as small-circular vesicles on a string or sand grains homogenously distributed and lined on a thread, and zein-gelatin polymers were red strings. The defects that were also seen in SEM images can also be seen in CLSM images as larger beads (white arrows) compared to the liposome vesicles. Additionally, the FE-SEM images taken with the STEM detector in Figure 4d, e confirmed the presence of embedded liposomes in the fiber, and the incorporation of liposomes into the core did not disrupt the core-shell structures of fibers. The mild processing conditions of the electrospinning process and tunable formulation of feed solutions enable the loading of bioactive compounds and liposomal structures into fibers.[58] Although in Figure 4e, the contrast was not enough between liposomes and polymers due to the lack of dye, the darker vesicles could still be superficially perceived (black arrows).

3.3 | Differential scanning calorimetric analysis of fibers

The DSC analysis was carried out as part of fiber characterization and to investigate the change in thermal properties of samples depending on the formulation. DSC thermograms of liposomal fibers and their ingredients, zein, gelatin, lecithin, and propolis were given in Figure 5. Lecithin showed an endothermic peak at 147.04 and 213.74°C due to melting and decomposition.[77] Pure gelatin thermograms showed water desorption between 70 and 100°C (73.06°C), and the transition between 150 and 200°C (149.67°C), those were also previously reported for gelatin.[78] The zein showed an endothermic melting peak at 156.47°C. In EF consisting of only zein and gelatin, the melting peak was shifted to 178.05°C indicating that fiber structure was thermally more stable than pure zein and gelatin.[48] Loading EF with blank (F4B) or PE-loaded liposomes (F2 and F4), all reduced the melting point. When EF was loaded with blank liposome (F4B), the melting peak was seen at a lower temperature (121.12°C). When this fiber was loaded with liposomal PE (F4), a sharp melting peak was seen at a higher temperature of 168.16°C which might indicate the presence of PE that was not previously encapsulated in liposomes.[79] Similarly, Ansarifar et al.,[80] and İnanç Horuz and Belibağlı[81] reported higher melting peaks of zein fibers when encapsulating the hydrophobic compounds such as thyme essential oil and carotenoids. The incorporation of blank liposomes or PE-loaded liposomes did not lead to the formation of more endothermic peaks, which indicates the miscibility of spinning solutions.[42]

3.4 | Fourier transform infrared spectra of fibers

Figure 6 showed the FTIR spectra of the liposomal PE-loaded fibers and the related ingredients used to prepare them. A broad band at 3350 cm^{-1} in PE occurs due to the O–H stretching vibration of the phenolic groups. The lecithin had a peak at 3010 cm^{-1} that could be ascribed to the asymmetric stretching vibration of the CH_3 groups related to the triglyceride moiety. The bands at 2925 and 2853 cm^{-1} correspond to asymmetric and symmetric C–H stretching vibrations which were observed both in PE and lecithin. These absorption bands of PE may be associated with wax residues. It was reported that the entrapment of propolis in the liposome phospholipid bilayer could result from the hydrophobic interactions between the aromatic rings of the propolis flavonoid and the phospholipid acyl chains.[82] A strong peak observed in lecithin at 1733 cm^{-1} which was related to the symmetric C=O ester vibrations, and the bands at 1234 and 1166 cm^{-1} were due to the PO_2 vibration, and the peaks at 1055 and 970 cm^{-1} were due to asymmetrical stretch vibrations of the choline group (N^+CH_3) belonging to the polar region of phosphatidylcholine.[83] The absorption bands of PE at 1701 and 1168 cm^{-1} indicate the presence of a carboxylic group and in all liposomal PE-loaded fibers it exerted itself at 1170 cm^{-1}. Specifically, the absorption band at 1701 cm^{-1} is related to stretching vibrations of carboxyl groups (–COOH), and two bands at

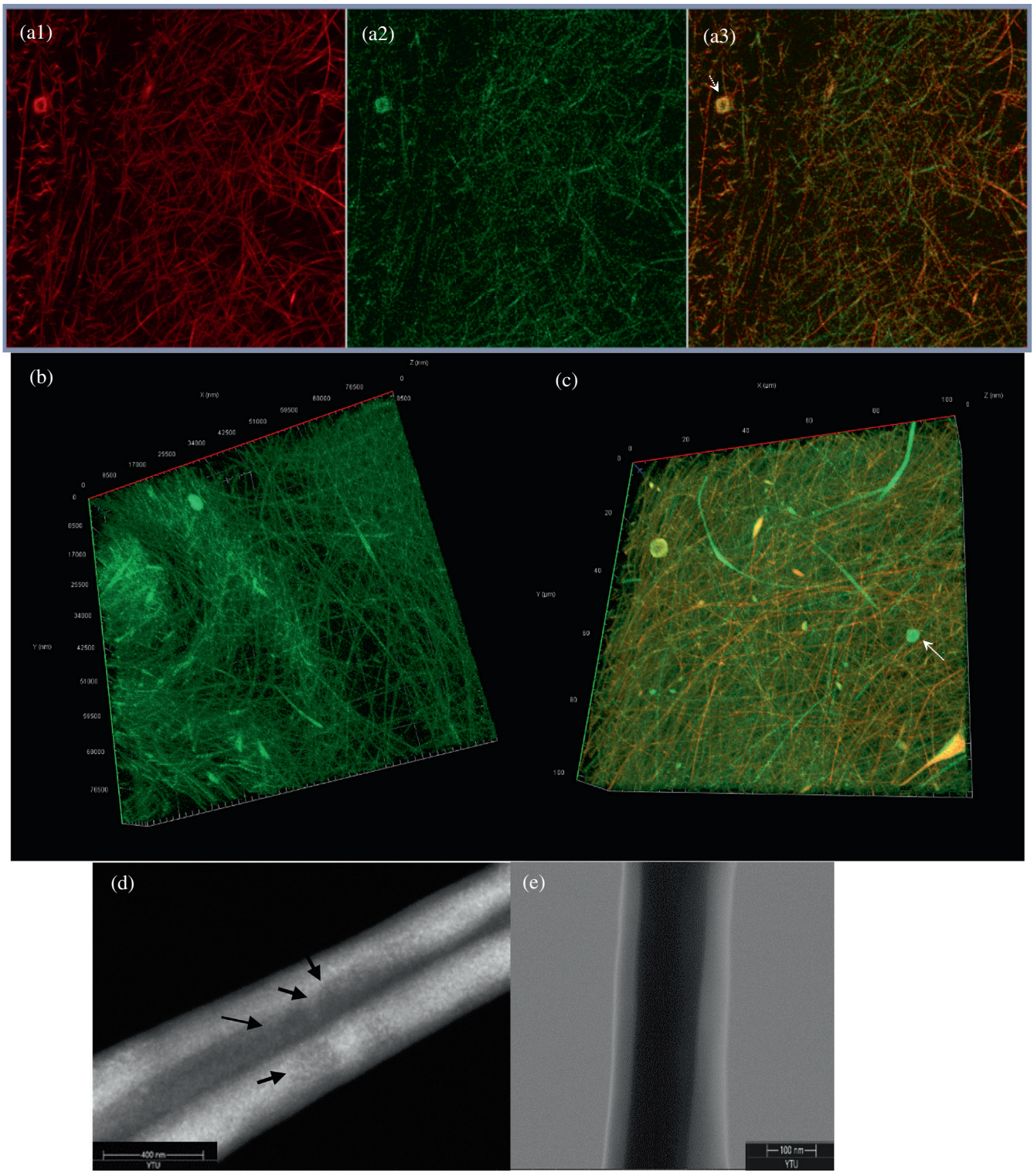

FIGURE 4 Confocal microscopy and scanning transmission electron microscopy (STEM) images of liposomal fiber (a1) Polymers stained with Fast Green, (a2) Liposomes stained with Nile Red, (a3) overlay image. (b) 3D image of liposomes in fiber, stained with Nile Red (c) 3D overlay image of liposomes in fiber, stained with Nile Red and Fast Green. Green and red colors were liposomes and polymers, respectively. (d) and (e) STEM images of core/shell structure of liposomal fiber. [Color figure can be viewed at wileyonlinelibrary.com]

1633 and 1600 cm^{-1} could be attributed to aromatic stretching vibrations of C=C and/or C=O groups due to amino acids and flavonoids. The band at 1512 cm^{-1} is related to the aromatic ring deformations of C=C stretching, and 1454 and 1377 cm^{-1} for C–H bending and aromatic C–O stretching vibrations.[42,64] The peak at

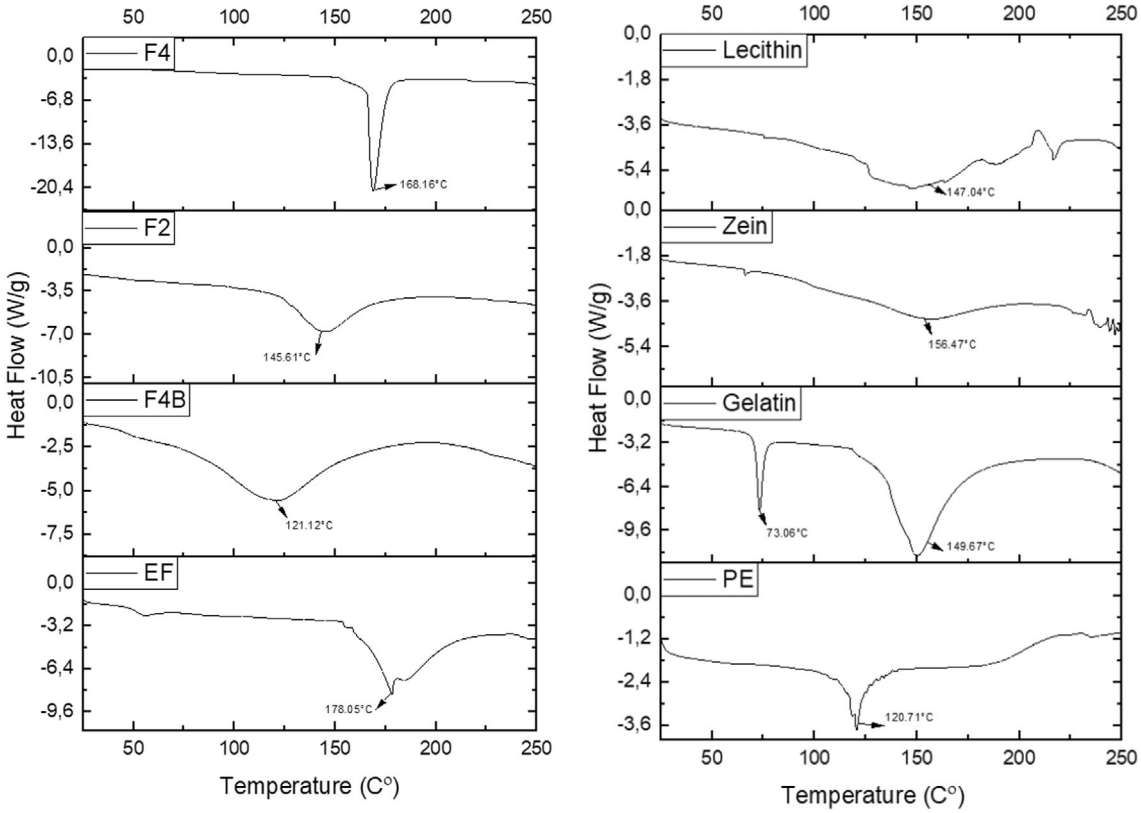

FIGURE 5 Differential scanning calorimetric thermograms of zein, gelatin, lecithin, propolis extract (PE); and liposomal PE-loaded fibers. F2 and F4: fibers loaded with liposomal PE (L2 and L4); F4B: fiber loaded with blank-PE free L4 liposome; EF: empty fiber (without liposomal PE, only polymers).

3303 cm^{-1} in zein and 3286 cm^{-1} in gelatin are due to O–H and N–H stretching and might be affected by the hydrogen bonding interactions between gelatin and zein, and it was centered at 3292 cm^{-1} in fibers.[84] Two absorption bands between 2852 and 2940 cm^{-1} are attributed to the C–H stretching vibrations of aliphatic groups of proteins, and centered at around 2959 cm^{-1} in fibers.[85] The characteristic absorption peaks for identifying gelatin and zein were at 1629 and 1635 cm^{-1} related to C=O stretching vibrations of amide I; at 1517 and 1521 cm^{-1} associated with N-H bending of amide II; at 1238 and 1234 cm^{-1} corresponded to amide III groups.[86] The main functional groups of proteins were shifted to 1652, 1538, and 1244 cm^{-1} in the spectra of liposomal PE-loaded fibers, which could indicate the interaction among the functional groups of the ingredients within the fiber.

3.5 | Swelling, degradation, and PE release properties of fibers

The swelling capacity of oral wound dressings gives an idea of the rate at which water has been absorbed by the polymeric films when exposed to the wound surface. Theoretically, swelling is favorable for mucoadhesion since it allows the mobility of polymer chains. However, excess swelling could lead to decreased retention in the mucus layer due to the formation of slippery mucilage and the remoteness of functional groups in polymers. The material should also be able to prolong the release of encapsulated active compounds and maintain its structural integrity over time.[87]

The swelling behavior of liposomal PE-loaded fiber (F4) was evaluated at two different pH levels (pH 4.5 and 7.5). The pH of the oral cavity ranged between 4 and 7.5 following the intake of fermentable carbohydrates, acidic liquids, or sugar in the presence of acidogenic bacteria, and after consumption of food, there was an elimination of the acid and a return to normal saliva.[88] In some cases, patients with gastroesophageal reflux disease also have oral cavities with pH values as low as 4.9,[89] and this condition frequently results in oral lesions.[90] In another example, the chronic and nonhealing oral wounds commonly observed in diabetic patients contributed to the formation of a local environment with a low pH value.[4]

The swelling ratio of the sample in PBS peaked (up to 40%) between 0 and 2 h, then reduced to around 25% (2–5 h), and increased to ∼ 38% in the remaining period

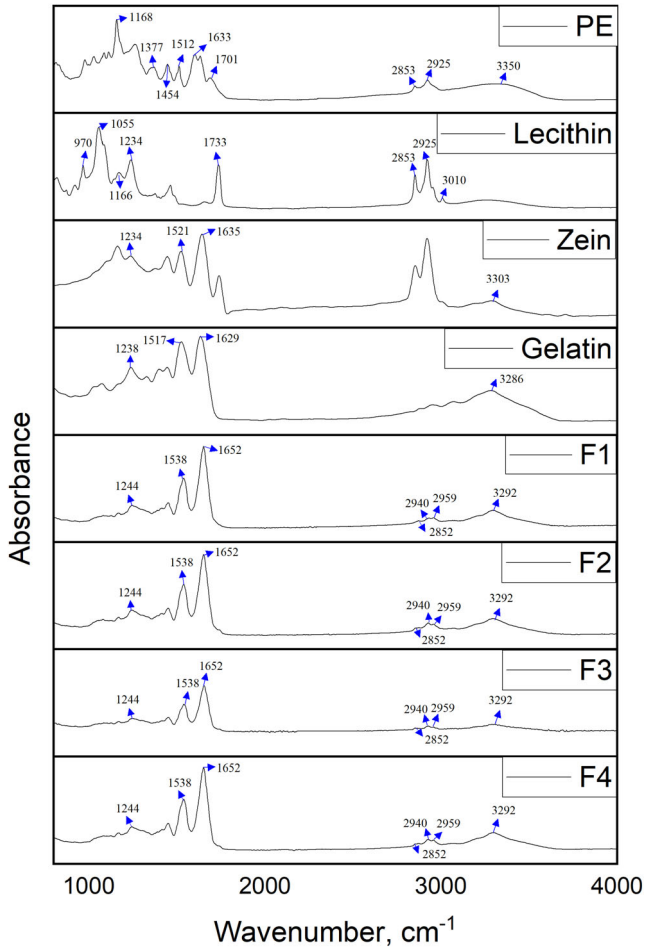

FIGURE 6 Fourier transform infrared spectra of zein, gelatin, lecithin, propolis extract (PE), and liposomal PE-loaded fibers. F1–F4: fibers loaded liposomal PE (L1–L4). [Color figure can be viewed at wileyonlinelibrary.com]

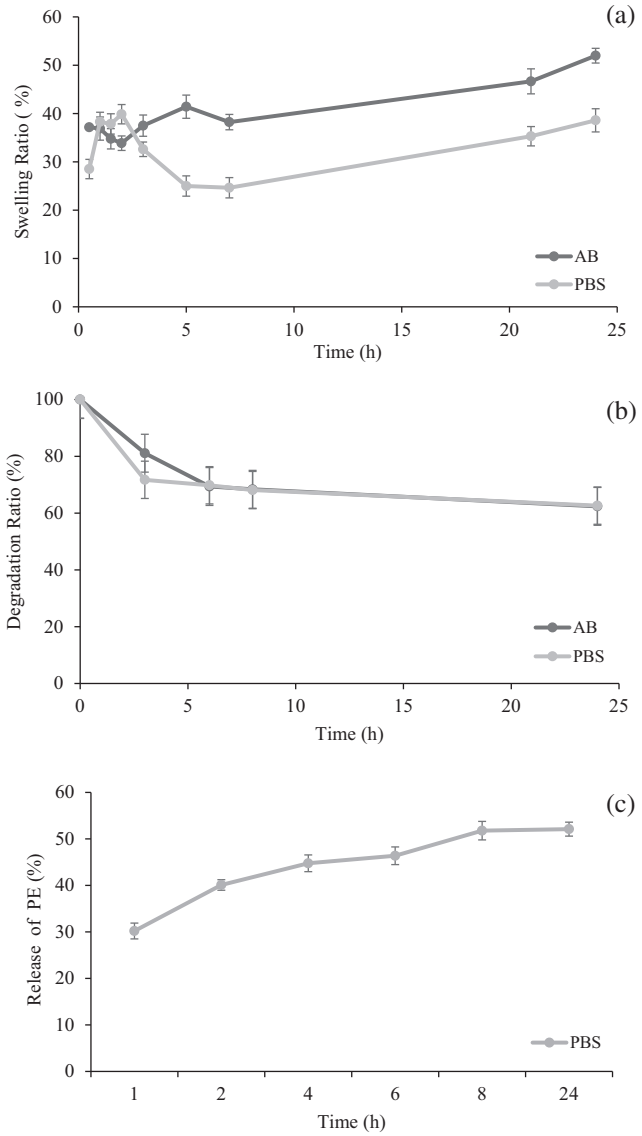

FIGURE 7 (a) Swelling ratio (%), (b) Degradation ratio (%), and (c) Release of propolis extract (PE) (%) of liposomal fiber (F4).

over a 24-h period. A higher swelling ratio of fiber was observed in AB, and the swelling ratio (37%) achieved in the first 30 min. of immersion was slightly reduced to ∼ 33% after 2 h, and the fiber continued to swell (up to 51%) in the following period (Figure 7a). Zein and gelatin are both proteins, but due to the presence of a high proportion of nonpolar amino acid residues, zein has a hydrophobic nature, whereas gelatin is highly hydrophilic and has a high swelling capacity.[91] The difference in the swelling behavior of fibers in PBS and AB could be explained by the hydrophobic character of zein and its higher solubility in an acidic medium. In PBS, gelatin was expected to be dissolute, whereas zein would be aggregated. The decrease in the swelling ratio of fibers would also be related to the degradation of fiber (20%–30%) mainly occurred in the first 3 h of immersion in both buffers and reached 38% after a 24-h period (Figure 7b).

When liposomal fiber was immersed in PBS, fiber structures could still be observed after 15 min, whereas in AB, the fiber structures fused together (Figure 8). 1 h later, the fiber was eroded in AB, whereas the erosion was less prominent in the PBS solution. At 6 h of immersion, the fibers in the AB were more eroded and openings of large pores were observed. At the end of 24 h, both mediums degraded the structures, but the AB medium was more detrimental. In the electrospinning process, the solvent is rapidly evaporated, and polymers (proteins) are expected to be solidified "layer by layer" from the outside to the inside depending on their affinity to the solvent (water) and/or air.[84] Since the solvent evaporated from the outer surface towards the center of the jet, it was anticipated that the proteins rich in hydrophilic groups would typically align with the polar interior (liquid/aqueous side), whereas proteins rich in hydrophobic groups

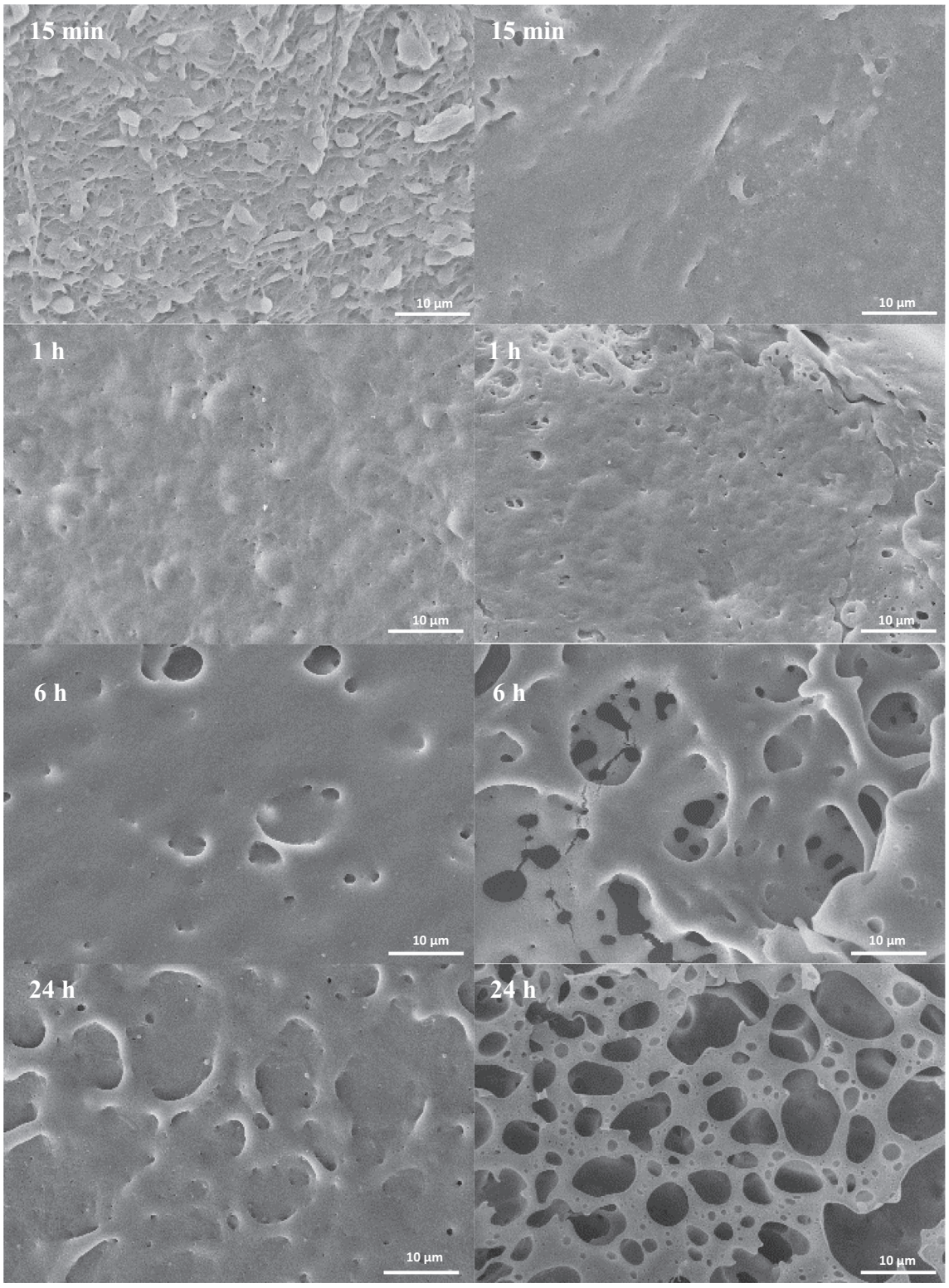

FIGURE 8 Microstructure of liposomal fiber (F4) immersed in phosphate buffer (PBS) (left) and acetate buffer (AB) (right) after 15 min, 1 h, 6 h, and 24 h.

would face outward (airside). The fiber sample could have a more hydrophobic component (zein) at the outer layers that contact the buffer first, whereas the more hydrophilic protein (gelatin) would be aligned in the inner layer, so this could affect the water absorption and structure of the fiber depending on the buffer and immersion period.

The release of PE from liposomal fiber was only investigated in the PBS (Figure 7c), as coincided with

swelling, degradation analysis, and SEM images, the release after 1 h was only ~30% of the initially loaded amount and reached 50% even after 24 h of immersion. The delayed release of bioactive compounds from swollen fibers/patches was also reported in previous studies.[92,93] As the fiber structure coalesced in the PBS over time, as evidenced by SEM micrographs (Figure 8), a slower release of PE was accompanied by the fibers over time.

3.6 | Mucoadhesion

Although one of the challenges for oral wound dressings is the secretion of saliva, the wetting conditions of the oral cavity bring the swellable polymer materials into close contact with the mucin, glycosylated peptides secreted into saliva, and the most important structure-forming component of the mucus, providing its gel-like, cohesive, and adhesive properties. A mucoadhesive formulation should aim to prolong the residence time of the drug on the site of application through interaction with the mucus layer.[94] The mucoadhesive strengths of the samples were determined by measuring the force required to detach fibers from hydrated mucin discs using the texture analyzer. In liposomal PE-loaded fibers (F1–F4), the mucoadhesion work ranged between 0.21 and 0.42 N mm. Compared to F1–F2 fibers, the F3 and F4 formulations with higher PE loading (Table 3) presented higher mucoadhesion work (Figure 9). The functional hydroxyl, carboxyl, or amine groups of the polymers were reported to favor adhesion with mucus, therefore, due to elevated PE content, F3–F4 fibers could exhibit a higher density of available hydrogen bonding groups to interact more strongly with mucin glycoproteins. Rosseto et al.[95] suggested that the enhanced bioadhesiveness of polymeric carbopol films loaded with PE was due to the resinous residues and hydrophobic character that may also contribute to the increased hydrophobic interactions between the films and mucosa.[96]

The incorporation of plasticizers could improve the flexibility and chain mobility of zein films by reducing strong hydrophobic intermolecular forces through hydrogen bonding interaction.[97] It was also suggested that the chain mobility/flexibility of the polymers was a critical for interpenetration and entanglement with the mucus gel. Increased chain mobility would lead to increased interdiffusion and interpenetration of the polymer within the mucus network and enhanced mucoadhesive properties.[87] It could be another reason for the elevated mucoadhesion provided by F3 and F4 fibers that were embedded with liposomes containing Tween 80 and a higher amount of lecithin compared to liposomes of F1 and F2 fibers.

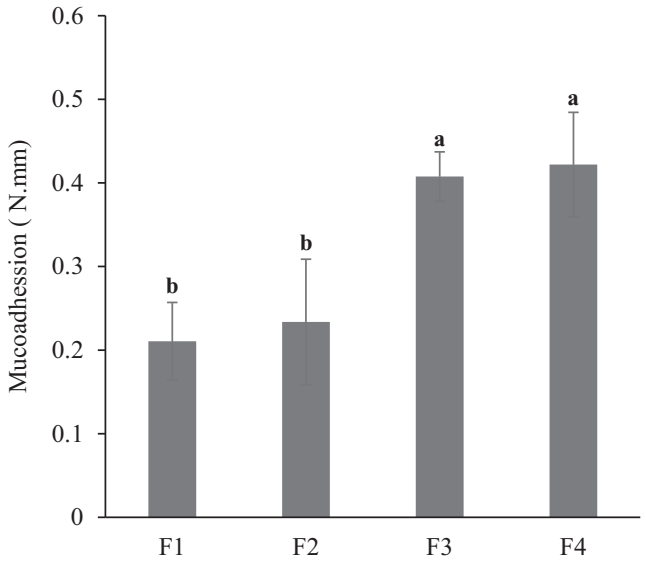

FIGURE 9 In vitro mucoadhesive property of liposomal propolis extract (PE)-loaded fibers. F1–F4: fibers loaded with liposomal PE (L1–L4). Values were presented as mean ± SD ($n = 6$), means with different letters were significantly different ($p < 0.05$).

3.7 | Antimicrobial analysis

The antibacterial activity of PE-loaded liposomal fiber (F4) was determined by disk diffusion assay (Figure 10). The blank liposomal fiber was analyzed as negative control. *E. coli* (gram-negative; ATCC 25922), *P. aeruginosa* (gram-negative; ATCC 27853), and *S. aureus* (gram-positive; ATCC 25023) are bacteria commonly found in skin wounds.[61–63] The greatest inhibition zone (11.33 ± 0.57 mm) was seen against *S. aureus*, followed by *P. aeruginosa* (8.33 ± 0.57 mm), and *E. coli* (7.33 ± 0.57 mm), respectively (Figure 10), with no zone formation in blank fibers. PE-loaded liposomal fiber showed higher antimicrobial activities against *S. aureus*, a gram-positive bacteria. It could be attributed to the outer membrane of gram-negative bacteria, which consists of lipopolysaccharides that inhibit and/or retard the penetration of the antimicrobial components of propolis.[43] The antimicrobial properties of PE have been mainly due to different components such as flavonoids and cinnamic acid derivatives. Flavonoids were known to interfere with the energy metabolism of bacterial cells due to damage to the cytoplasmatic membranes, altering their permeability, and perturbing the exchange of nutrients and metabolites.[8]

3.8 | MTT assay

The MTT cytotoxicity test gives information about the biocompatibility of a material, its effect on the

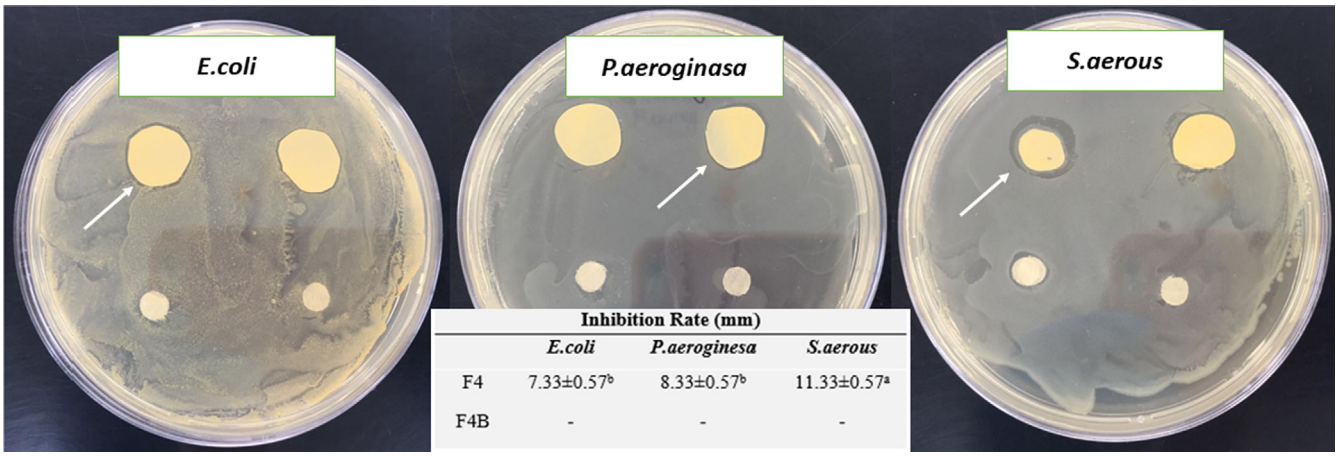

FIGURE 10 The inhibition zones of liposomal propolis extract (PE)-loaded fiber (F4) against *Escherichia coli* (gram-negative, ATCC 25922), *Pseudomonas aeruginosa* (gram-negative, ATCC 27853), and *Staphylococcus aureus* (gram-positive, ATCC 29213) incubation at 37°C for 24 h. Values were presented as mean ± SD ($n = 6$), means with different letters were significantly different ($p < 0.05$). [Color figure can be viewed at wileyonlinelibrary.com]

proliferation rate of cells, and the metabolic activities of cells.[98] The cytotoxicity effects of liposomal PE embedded fibers (F3 and F4), blank liposome embedded fibers (F4B), and positive control on HFF-1 cells were given in Figure 11. Zein and gelatin have been shown to be biocompatible polymers,[84,99] and in our study, more than 50% of the cells remained viable in PE-free liposomal fiber (F4B). The loading of PE increased the cell viability, and the fiber with the highest PE loading (F4) showed higher viability (90.4%) ($p < 0.05$) compared to those of F3 (67.3%) and F4B (53.4%) (Figure 11), indicating that fibers with liposomal PE exhibited the ability to support cell proliferation. The components of propolis, such as flavonoids, phenolic acids, and their esters, could alleviate cell damage in fibroblast cells by suppressing intercellular reactive oxygen species production, and propolis was also reported to stimulate epithelial regeneration and modulate extracellular matrix deposition.[7] Similarly, the results of the cytotoxicity tests performed on human normal fibroblast cells (HFB4) for PE loaded-fiber embedded in PVA porous hydrogel suggested enhanced cell growth due to PE inclusion.[100] The niosomal-loaded silk fibroin fibers increased the proliferation of L929 mouse fibroblast cells in the presence of propolis.[46]

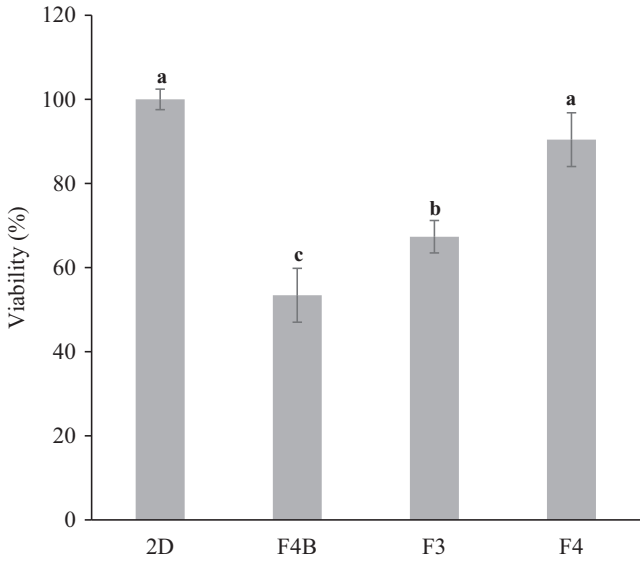

FIGURE 11 MTT test results of HFF-1 fibroblast cells. F3 and F4: fibers loaded liposomal propolis extract (PE) (L3 and L4); F4B: fiber loaded with blank-PE free L4 liposome; 2D: the positive control. Values were presented as mean ± SD ($n = 3$). Means with different letters were significantly different ($p < 0.05$).

3.9 | Cell adhesion on liposomal fiber

Cell adhesion and distribution of fibroblasts on F4 fiber after 24 h of incubation in the medium was verified by SEM images (Figure 12). When evaluated together with the MTT test results (Figure 11), liposomal fiber may provide an efficient platform for the growth of the fibroblast cells. The seeded cells have a rounded shape, which may be caused by dehydration during the fixation process.[100] Moreover, the cells were seen contacting neighboring ones, spreading, and lining-up satisfactorily on the surfaces of the fiber (Figure 12). These data are in agreement with the studies of de Figueiredo et al.[40] who found that propolis and polymer-based fibers and films promote the migration of fibroblast cells.

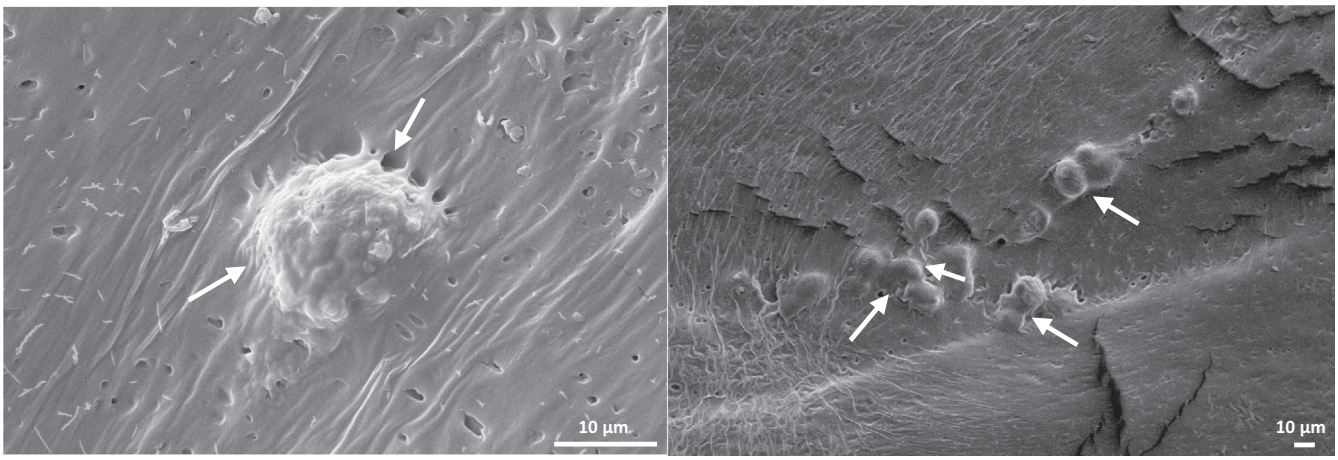

FIGURE 12 Scanning electron microscopy images of HFF-1 cells grown on liposomal propolis extract (PE)-loaded fiber (F4).

4 | CONCLUSION

Propolis-loaded soy-phosphatidylcholine liposomes were produced by thin-film hydration and ultrasonication method. Tween 80 was added to liposome formulations to improve the loading ratio of PE. In the production of coaxial fibers by electrospinning, liposomal PE was used as the core material, and zein/gelatin was applied as the shell material. Liposomes preserved their structure when embedded in fiber, as evidenced by CLSM and FE-SEM. Fibers loaded with PE-loaded liposomes provided lower TS and higher EAB values, which could indicate the improved flexibility and elasticity of fibers. The fibers loaded with liposome formulations enabling higher PE loading exhibited elevated mucoadhesion. The liposomal fiber displayed a lower swelling ratio and erosion in PBS compared to an acidic medium. The amount of PE released from the fibers reached around 50% of the initial loading, and the degradation of the fibers was only 30% after 6 h of incubation in PBS. The liposomal PE-loaded core/shell fiber demonstrated antimicrobial activity, its biocompatibility was confirmed by cell viability, and fibroblast cells were attached to the fiber, and therefore it could be suggested as a potential wound healing material. Integration of the liposomal fibers with anionic character in the cast films of cationic food-grade polymers with tunable mucoadhesive and release properties could be studied in the future, and this work can be taken forward for in vivo oral wound healing applications.

AUTHOR CONTRIBUTIONS

Canan Yagmur Karakas: Data curation (lead); supervision (lead); writing – original draft (lead); writing – review and editing (lead). **Cem Bulent Ustundag:** Conceptualization (supporting); investigation (supporting); methodology (supporting); validation (supporting). **Ali Sahin:** Conceptualization (supporting); investigation (supporting); methodology (supporting); validation (supporting). **Ayse Karadag:** Conceptualization (lead); data curation (lead); investigation (lead); methodology (lead); supervision (lead); validation (lead); writing – original draft (lead); writing – review and editing (lead).

ACKNOWLEDGMENTS

This research was supported by The Scientific and Technological Research Council of Turkey, TUBITAK (grant number 120O315). Canan Yagmur Karakas was supported by the 100/2000 Ph.D. scholarship program of the Council of Higher Education (CoHE) and 2211-A of TUBITAK. The authors also thanks to Balparmak (Altıparmak Gıda, İstanbul, Turkey).

DATA AVAILABILITY STATEMENT

The data that support the findings of this study are available from the corresponding author upon reasonable request.

ORCID

Canan Yagmur Karakas https://orcid.org/0000-0002-9653-5557
Ali Sahin https://orcid.org/0000-0001-5594-1551
Ayse Karadag https://orcid.org/0000-0001-8615-7321

REFERENCES

[1] S. Jongjitaree, S. Koontongkaew, N. Niyomtham, B. E. Yingyongnarongkul, K. Utispan, *Evid. Based Complement. Alternat. Med.* **2022**, *2022*, 3503164.
[2] K. M. Galler, M. Weber, Y. Korkmaz, M. Widbiller, M. Feuerer, *Int. J. Mol. Sci.* **2021**, *22*, 1.
[3] B. Marques Vieira, N. D. de Almeida Neto, L. E. Simões, E. J. Feres-Filho, M. I. C. Gaspar-Elsas, P. Xavier-Elsas, *Int. Immunopharmacol.* **2022**, *105*, 108544.

[4] J. Sun, T. Chen, B. Zhao, W. Fan, Y. Shen, H. Wei, M. Zhang, W. Zheng, J. Peng, J. Wang, Y. Wang, L. Fan, Y. Chu, L. Chen, C. Yang, *ACS Appl. Mater. Interfaces* **2022**, *15*, 416.
[5] J. C. Silva, S. Rodrigues, X. Feás, L. M. Estevinho, *Food Chem. Toxicol.* **2012**, *50*, 1790.
[6] A. Eskandarinia, M. Rafienia, S. Navid, M. Agheb, *J. Polym. Environ.* **2018**, *26*, 3345.
[7] G. T. Voss, M. S. Gularte, A. G. Vogt, J. L. Giongo, R. A. Vaucher, J. V. Z. Echenique, M. P. Soares, C. Luchese, E. A. Wilhelm, A. R. Fajardo, *Int. J. Pharm.* **2018**, *552*, 340.
[8] I. A. Freires, S. M. de Alencar, P. L. Rosalen, *Eur. J. Med. Chem.* **2016**, *110*, 267.
[9] O. Magro-Filho, A. C. de Carvalho, *J. Nihon Univ. Sch. Dent.* **1994**, *36*, 102.
[10] F. Zulhendri, R. Felitti, J. Fearnley, M. Ravalia, *J. Oral Biosci.* **2021**, *63*, 23.
[11] P. R. Barroso, R. Lopes-Rocha, E. M. F. Pereira, S. A. Marinho, J. L. de Miranda, N. L. Lima, F. D. Verli, *Inflammopharmacology* **2012**, *20*, 289.
[12] M. G. Arafa, D. Ghalwash, D. M. El-Kersh, M. M. Elmazar, *Sci. Rep.* **2018**, *8*, 1.
[13] P. Mendez-Pfeiffer, J. Juarez, J. Hernandez, P. Taboada, C. Virués, D. Valencia, C. Velazquez, *J. Drug Deliv. Sci. Technol.* **2021**, *65*, 102762.
[14] V. Tzankova, D. Aluani, Y. Yordanov, M. Kondeva-Burdina, P. Petrov, V. Bankova, R. Simeonova, V. Vitcheva, F. Odjakov, A. Apostolov, B. Tzankov, K. Yoncheva, *Rev. Bras. Farmacogn.* **2019**, *29*, 364.
[15] H. Zhang, Y. Fu, F. Niu, Z. Li, C. Ba, B. Jin, G. Chen, X. Li, *Food Hydrocoll.* **2018**, *81*, 104.
[16] M. Li, C. Du, N. Guo, Y. Teng, X. Meng, H. Sun, S. Li, P. Yu, H. Galons, *Eur. J. Med. Chem.* **2019**, *164*, 640.
[17] Q. Li, H. Lin, J. Li, L. Liu, J. Huang, Y. Cao, T. Zhao, D. J. McClements, J. Chen, C. Liu, J. Liu, P. Shen, M. Zhou, *Food Hydrocoll.* **2023**, *134*, 108028.
[18] C. Tan, J. Wang, B. Sun, *Biotechnol. Adv.* **2021**, *48*, 107727.
[19] T. Klemetsrud, H. Jonassen, M. Hiorth, A. L. Kjøniksen, G. Smistad, *Colloids Surf. B Biointerface* **2013**, *103*, 158.
[20] H. He, Y. Lu, J. Qi, Q. Zhu, Z. Chen, W. Wu, *Acta Pharm. Sin. B* **2019**, *9*, 36.
[21] A. Karadag, B. Özçelik, M. Sramek, M. Gibis, R. Kohlus, J. Weiss, *J. Food Sci.* **2013**, *78*, E206.
[22] R. H. de Freitas Zômpero, A. López-Rubio, S. C. de Pinho, J. M. Lagaron, L. G. de la Torre, *Colloids Surf. B Biointerface* **2015**, *134*, 475.
[23] C. Valencia-Sullca, M. Jiménez, A. Jiménez, L. Atarés, M. Vargas, A. Chiralt, *Polym. Int.* **2016**, *65*, 979.
[24] Y. Xu, Y. Chu, X. Feng, C. Gao, D. Wu, W. Cheng, L. Meng, Y. Zhang, X. Tang, *Int. J. Biol. Macromol.* **2020**, *156*, 111.
[25] K. Hasanbegloo, S. Banihashem, B. Faraji Dizaji, S. Bybordi, N. Farrokh-Eslamlou, P. G. Abadi, F. S. Jazi, M. Irani, *Int. J. Biol. Macromol.* **2023**, *230*, 123380.
[26] K. Feng, C. Li, Y.-S. Wei, M.-H. Zong, H. Wu, S.-Y. Han, *J. Colloid Interface Sci.* **2019**, *552*, 186.
[27] S. Amjadi, H. Almasi, M. Ghorbani, S. Ramazani, *Food Packag. Shelf. Life* **2020**, *24*, 100504.
[28] A. Mickova, M. Buzgo, O. Benada, M. Rampichova, Z. Fisar, E. Filova, M. Tesarova, D. Lukas, E. Amler, *Biomacromolecules* **2012**, *13*, 952.
[29] A. Alehosseini, L. G. Gómez-Mascaraque, M. Martínez-Sanz, A. López-Rubio, *Food Hydrocoll.* **2019**, *87*, 758.
[30] M. Surendranath, R. M. Ramesan, P. Nair, R. Parameswaran, *Mol. Pharm.* **2023**, *20*, 508.
[31] A. Ahmady, N. H. Abu Samah, *Int. J. Pharm.* **2021**, *608*, 121037.
[32] X. Li, Z. C. Tu, X. M. Sha, Y. H. Ye, Z. Y. Li, *Food Sci. Nutr.* **2020**, *8*, 3099.
[33] S. Dede, O. Sadak, M. Didin, S. Gunasekaran, *Food Packag. Shelf Life* **2023**, *35*, 101035.
[34] A. E. Torkamani, Z. A. Syahariza, M. H. Norziah, A. K. M. Wan, P. Juliano, *Food Biosci.* **2018**, *21*, 60.
[35] W. Yang, A. M. M. Sousa, X. Fan, T. Jin, X. Li, P. M. Tomasula, L. Liu, *Carbohydr. Polym.* **2017**, *157*, 1173.
[36] C. Yao, B. Zhou, Y. Miao, X. Liu, *Text. Res. J.* **2016**, *86*, 1023.
[37] R. Bilginer, D. Ozkendir-Inanc, U. H. Yildiz, A. Arslan-Yildiz, *J. Appl. Polym. Sci.* **2021**, *138*, 50287.
[38] M. S. Morais, D. P. F. Bonfim, M. L. Aguiar, W. P. Oliveira, *J. Pharm. Innov.* **2022**, *17*, 1.
[39] M. S. Mirbagheri, S. Akhavan-Mahdavi, A. Hasan, M. S. Kharazmi, S. M. Jafari, *Int. J. Pharm.* **2023**, *642*, 123186.
[40] A. C. de Figueiredo, J. M. Anaya-Mancipe, A. O. de Barros, R. Santos-Oliveira, M. L. Dias, R. M. da Thiré, *Molecules* **2022**, *27*, 27.
[41] R. Mohamadinooripoor, S. Kashanian, P. Moradipour, S. Sajadimajd, E. Arkan, A. Tajehmiri, K. Rashidi, *J. Polym. Res.* **2022**, *29*, 29.
[42] B. M. Razavizadeh, R. Niazmand, *Heliyon* **2020**, *6*, e04784.
[43] L. Moradkhannejhad, M. Abdouss, N. Nikfarjam, S. Mazinani, V. Heydari, *J. Mater. Sci. Mater. Med.* **2018**, *29*, 29.
[44] S. Hochheim, N. M. F. M. Sampaio, A. F. da Cruz, L. L. del Mercato, E. D'Amone, B. J. G. da Silva, C. K. Saul, C. C. de Oliveira, I. Riegel-Vidotti, *Macromol. Biosci.* **2023**, *23*, 2200524.
[45] I. Bonadies, F. Cimino, V. Guarino, *Mater. Res. Express* **2019**, *6*, 75407.
[46] M. Behyari, R. Imani, H. Keshvari, *Fibers Polym.* **2021**, *22*, 2090.
[47] X. R. Shao, X. Q. Wei, S. Zhang, N. Fu, Y. F. Lin, X. X. Cai, Q. Peng, *Nanoscale Res. Lett.* **2017**, *12*, 12.
[48] M. Gültekin-Özgüven, A. Karadağ, Ş. Duman, B. Özkal, B. Özçelik, *Food Chem.* **2016**, *201*, 205.
[49] V. L. Singleton, J. A. Rossi, *Am. J. Enol. Vitic.* **1965**, *16*, 144.
[50] A. Meda, C. E. Lamien, M. Romito, J. Millogo, O. G. Nacoulma, *Food Chem.* **2005**, *91*, 571.
[51] A. Pękal, K. Pyrzynska, *Food Anal. Methods* **2014**, *7*, 1776.
[52] K. S. Hiray, P. K. Suresh, *Ind. J. Pharm. Educ. Res.* **2020**, *54*, S182.
[53] X. Li, Z. Ren, R. Wang, L. Liu, J. Zhang, F. Ma, M. Z. H. Khan, D. Zhao, X. Liu, *Food Chem.* **2021**, *349*, 129208.
[54] X. Xu, Y. Shen, W. Wang, C. Sun, C. Li, Y. Xiong, J. Tu, *Eur. J. Pharm. Biopharm.* **2014**, *88*, 998.
[55] F. G. Prezotti, I. Siedle, F. I. Boni, M. Chorilli, I. Müller, B. S. F. Cury, *Pharm. Dev. Technol.* **2020**, *25*, 159.
[56] F. Ciftci, S. Ayan, N. Duygulu, Y. Yilmazer, Z. Karavelioglu, M. Vehapi, R. Cakır Koc, M. Sengor, H. Yılmazer, D. Ozcimen, O. Gunduz, C. B. Ustundag, *Int. J. Polym. Mater. Polym. Biomater.* **2022**, *71*, 898.
[57] G. D. Zhao, R. Sun, S. L. Ni, Q. Xia, *J. Microencapsul.* **2015**, *32*, 157.
[58] C. Li, M. Bai, X. Chen, W. Hu, H. Cui, L. Lin, *Food Biosci.* **2022**, *46*, 101578.

[59] C. Tan, J. Xue, S. Abbas, B. Feng, X. Zhang, S. Xia, *J. Agric. Food Chem.* **2014**, *62*, 6726.
[60] S. Xia, S. Xu, *Food Res. Int.* **2005**, *38*, 289.
[61] K. Tai, X. He, X. Yuan, K. Meng, Y. Gao, F. Yuan, *Colloids Surf. A Physicochem. Eng. Asp.* **2017**, *518*, 218.
[62] B. Romana, M. M. Hassan, F. Sonvico, G. Garrastazu Pereira, A. F. Mason, P. Thordarson, K. E. Bremmell, T. J. Barnes, C. A. Prestidge, *Eur. J. Pharm. Biopharm.* **2020**, *154*, 338.
[63] A. A. Aytekin, S. Tuncay Tanrıverdi, F. Aydın Köse, D. Kart, İ. Eroğlu, Ö. Özer, *J. Liposome Res.* **2020**, *30*, 107.
[64] N. A. Ramli, N. Ali, S. Hamzah, N. I. Yatim, *Heliyon* **2021**, *7*, e06649.
[65] M. Gibis, E. Vogt, J. Weiss, *Food Funct.* **2012**, *3*, 246.
[66] S. Toro-Uribe, E. Ibáñez, E. A. Decker, D. J. McClements, R. Zhang, L. J. López-Giraldo, M. Herrero, *J. Agric. Food Chem.* **2018**, *66*, 12051.
[67] B. Guldiken, A. Linke, E. Capanoglu, D. Boyacioglu, R. Kohlus, J. Weiss, M. Gibis, *J. Food Eng.* **2019**, *246*, 42.
[68] M. Frenzel, A. Steffen-Heins, *Food Chem.* **2015**, *185*, 48.
[69] J. Yuan, Y. Lu, S. Abula, Y. Hu, J. Liu, Y. Fan, X. Zhao, D. Wang, X. Liu, C. Liu, *Evid. Based Complement. Altern. Med.* **2013**, *2013*, 505703.
[70] M. Preis, K. Knop, J. Breitkreutz, *Int. J. Pharm.* **2014**, *461*, 22.
[71] A. Rohani Shirvan, A. Bashari, N. Hemmatinejad, *Eur. Polym. J.* **2019**, *119*, 541.
[72] G. A. Ilevbare, H. Liu, K. J. Edgar, L. S. Taylor, *Cryst. Growth des.* **2012**, *12*, 6050.
[73] S. M. Gonçalves, D. C. dos Santos, J. F. G. Motta, R. R. dos Santos, D. W. H. Chávez, N. R. de Melo, *Carbohydr. Polym.* **2019**, *209*, 190.
[74] D. Wei, F. Zhou, H. Wang, G. Liu, J. Fang, Y. Jiang, *Materials (Basel)* **2022**, *15*, 2795.
[75] Y. Ge, J. Tang, H. Fu, Y. Fu, Y. Wu, *Fibers Polym.* **2019**, *20*, 698.
[76] H. Cui, M. Bai, C. Li, R. Liu, L. Lin, *LWT* **2018**, *96*, 671.
[77] S. Vedovatto, J. C. Facchini, R. K. Batista, T. C. Paim, M. I. Z. Lionzo, M. R. Wink, *Int. J. Biol. Macromol.* **2020**, *160*, 750.
[78] X. Wang, Z. Luo, Z. Xiao, *Carbohydr. Polym.* **2014**, *101*, 1027.
[79] S. Ali, Z. Khatri, K. W. Oh, I.-S. Kim, S. H. Kim, *Macromol. Res.* **2014**, *22*, 971.
[80] E. Ansarifar, F. Moradinezhad, *Int. J. Food Sci. Technol.* **2021**, *56*, 4239.
[81] T. İnanç Horuz, K. B. Belibağlı, *Food Chem.* **2018**, *268*, 86.
[82] D. Lombardo, P. Calandra, D. Barreca, S. Magazù, M. A. Kiselev, *Nanomaterials* **2016**, *6*, 6.
[83] O. Saroglu, B. Atalı, R. M. Yıldırım, A. Karadag, *J. Food Meas. Charact.* **2022**, *16*, 4402.
[84] L. Deng, Y. Li, F. Feng, H. Zhang, *Food Hydrocoll.* **2019**, *87*, 1.
[85] X. Wu, Z. Liu, S. He, J. Liu, W. Shao, *Food Chem.* **2023**, *426*, 136652.
[86] D. Wang, J. Sun, J. Li, Z. Sun, F. Liu, L. Du, D. Wang, *Food Chem.* **2022**, *373*, 131439.
[87] G. P. Andrews, T. P. Laverty, D. S. Jones, *Eur. J. Pharm. Biopharm.* **2009**, *71*, 505.
[88] W. H. Bowen, *Odontology* **2013**, *101*, 2.
[89] N. Kawar, S. G. Park, J. L. Schwartz, N. Callahan, A. Obrez, B. Yang, Z. Chen, G. R. Adami, *Sci. Rep.* **2021**, *11*, 1.
[90] L. Shu, X. Tong, *Front. Genet.* **2022**, *13*, 1.
[91] S. R. Falsafi, H. Rostamabadi, E. Assadpour, S. M. Jafari, *Adv. Colloid Interface Sci.* **2020**, *280*, 102166.
[92] S. Wongsasulak, S. Pathumban, T. Yoovidhya, *J. Food Eng.* **2014**, *120*, 110.
[93] K. Aranci, M. Uzun, S. Su, S. Cesur, S. Ulag, A. Amin, M. M. Guncu, B. Aksu, S. Kolayli, C. B. Ustundag, J. C. Silva, D. Ficai, A. Ficai, O. Gunduz, *Molecules* **2020**, *25*, 25.
[94] V. F. Patel, F. Liu, M. B. Brown, *J. Control. Release* **2011**, *153*, 106.
[95] H. C. Rosseto, L. de Alcântara Sica, R. de Toledo, L. M. B. Said dos Santos, C. F. de Francisco, E. Vecchi, R. Esposito, M. L. Cortesi, *J. Mol. Liq.* **2021**, *322*, 114514.
[96] J. G. Borges, R. A. de Carvalho, *J. Pharm. Sci.* **2015**, *104*, 1431.
[97] S. Tortorella, M. Maturi, V. Vetri Buratti, G. Vozzolo, E. Locatelli, L. Sambri, M. Comes Franchini, *RSC Adv.* **2021**, *11*, 39004.
[98] G. Ciapetti, E. Cenni, L. Pratelli, A. Pizzoferrato, *Biomaterials* **1993**, *14*, 359.
[99] N. Mamidi, I. L. Romo, H. M. Leija Gutiérrez, E. V. Barrera, A. Elías-Zúñiga, *MRS Commun.* **2018**, *8*, 885.
[100] S. Saleh, A. Salama, A. M. Ali, A. K. Saleh, B. A. Elhady, E. Tolba, *Sci. Rep.* **2023**, *13*, 7739.

How to cite this article: C. Y. Karakas, C. B. Ustundag, A. Sahin, A. Karadag, *J. Appl. Polym. Sci.* **2023**, e54683. https://doi.org/10.1002/app.54683